Theor Chim Acta (1992) 82: 383–396

Theoretica Chimica Acta

Simultaneous reptation and constraint release in polymer melts

N. A. Rotstein[1], S. Prager[1], T. P. Lodge[1], and M. Tirrell[2]

[1] Department of Chemistry, University of Minnesota, Minneapolis, MN 55455, USA

[2] Department of Chemical Engineering and Materials Science, University of Minnesota, Minneapolis, MN 55455, USA

Received March 3, 1991/Accepted June 10, 1991

Summary. A numerical solution to the parallel processes model for combined reptation and constraint release in polymer melts is presented. The discrete chain solution to the problem exhibits an exponent of 3 in the molecular weight dependence of the viscosity, just as in the strict reptation case; the magnitude of the viscosity is overestimated and no crossover to reptation is observed, as in Graessley's independent processes model. It is shown that linear combinations of reptation and constraint release, as modeled here, cannot describe the viscosity results observed experimentally.

Key words: Reptation – Constraint release – Viscosity – Entanglement phenomenon

1. Introduction

The entanglement phenomenon is one of the central problems in the dynamics of polymer liquids. In the past two decades considerable effort has been spent in developing theories based on the reptation hypothesis, that is, the idea that an entangled chain is constrained by neighboring chains to move predominantly along its own contour, as though it were trapped in a tube [1–3]. In a recent publication, both reptation-based and non-reptation models were reviewed and a thorough comparison with experimental data and computer simulations was conducted [4]. It was concluded that reptation models could provide an excellent overall description of polymer melt dynamics. However, some difficulties remain. An example of great interest is the molecular weight dependence of the zero shear rate viscosity. The reptation model both overestimates the magnitude and predicts a weaker molecular weight dependence: specifically, $\eta_{re} \sim M^3$ and $\eta_{ex} \sim M^{3.4}$ and $\eta_{re} > \eta_{ex}$, where η_{re} and η_{ex} are the predicted and experimental viscosities, respectively. The original theory of reptation (RE) was intended as a description of the dynamics of a single chain surrounded by a matrix of fixed obstacles [1]. In a polymer liquid, however, neighboring chains are mobile and as a result pure RE is presumed to provide a lower bound to the rates of chain diffusion and relaxation [5]. This matrix mobility can also make a significant

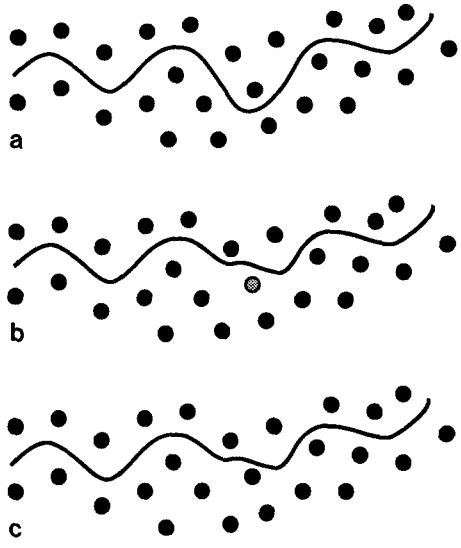

Fig. 1. **a** Schematic diagram of a 2-dimensional "slice" cut across the plane of a test chain. The *black filled circles* represent neighboring or matrix chains that are coming in and out of the plane of the test chain represented by the black line. **b** The *unfilled circle* represents a matrix chain end reptating past the test chain, releasing a constraint and allowing the test chain to make a lateral change in configuration. **c** Schematic of the new configuration of the test chain, the unfilled circle or chain end now replaced by a black one or matrix chain

contribution in polydisperse systems, and especially in binary blends of monodisperse polymers with widely separated molecular weights [4, 6–10].

Constraint release (CR) is an extension of the strict RE hypothesis to polymer liquids, which recognizes that the matrix constraining a chain to longitudinal motion is also made up of chains that are reptating [4, 5, 11, 12]. When a matrix chain end reptates past the test chain, a constraint is released and the test chain gains some lateral freedom (see Fig. 1). A combination of CR with RE was developed by Graessley, who made the assumption that the two mechanisms act independently [5]. For example, if $G_{CR}(t)$ and $G_{RE}(t)$ are the stress relaxation moduli for the pure CR and RE processes, respectively, $G(t)$ can be expressed as a simple product of both functions; thus, this model will be referred to as the independent processes model (IPM). This assumption has been utilized by other authors, for example Rubinstein and Colby, and it is of interest to investigate its validity [8].

In general $G(t)$ is related to the orientation correlation function $S(i, j; t)$, which gives the correlation between the orientations of subchain units i and j at time t. From this quantity we can obtain the subchain orientation autocorrelation function, $S(i, i; t)$ (also called the orientation function) by setting $i = j$ [2]. Watanabe and Tirrell have proposed the so-called configuration-dependent constraint release model, CDCR, as an alternative to the IPM [13]. This model analyzes the problem through the orientation function, assuming that both CR and RE processes are occurring in parallel in the time evolution equation for $S(i, j; t)$; this type of model will be referred to as the parallel processes model (PPM). It should be noted that neither the IPM nor the PPM take contour length fluctuations (or any other additional postulated relaxation mechanisms) into account [4, 5, 14].

Generally, linear polymers can be modeled as chains of N subunits, where N is proportional to the molecular weight of the polymer [4]. In this case i and j are discrete variables and we will refer to this level of description as the "discrete chain model". It is also common practice to consider the large N limit, where i and j can be taken to be continuous variables. This level of description will be

referred to as the "continuum limit approximation". In models for entangled polymers, N is often taken as M/M_e, where M_e is the molecular weight between entanglements (for example, as determined from the plateau modulus) [15]. As a result, the experimentally accessible region extends only to relatively low values of N, on the order of 10^2, and the validity of the continuum limit approximation must be examined. Watanabe and Tirrell solved the PPM problem analytically in the continuum limit by approximating $S(i, i; t)$ as a linear combination of the diagonal parts of the Rouse eigenfunctions, the so-called diagonal dominance approximation (DDA). In general, PPM predictions were found to be in better agreement with experiment than IPM predictions for a variety of viscoelastic properties at this level of description. In this paper we rederive the PPM and extend the previous work by solving the problem numerically, both for the discrete chain and in the continuum limit approximation. We compare both results and also compare the PPM to the IPM predictions and to experiment.

2. Theory

Definitions and assumptions

We adopt a chain consisting of N freely-jointed Gaussian subchains connecting $N+1$ beads. These subchains behave as entropic springs that follow Hooke's law and have zero rest length, so that:

$$\boldsymbol{f}_i = k\boldsymbol{r}_i \tag{1}$$

where $\boldsymbol{f}_i$ is the tension in the ith subchain, $\boldsymbol{r}_i$ its end-to-end vector, and $k = 3k_B T/r^2$ is the subchain force constant, where k_B is Boltzmann's constant, T is the temperature and r^2 is the equilibrium mean square end-to-end length of a subchain. The equilibrium distribution function for the chain is then:

$$\psi_{eq} \sim \exp\left(-k \sum_{i=1}^{n} r_i^2 / 2k_B T\right) \tag{2}$$

The stress $\sigma(t) \cdot \boldsymbol{n}$ across a plane normal to the $\boldsymbol{n}$-direction in a relaxing polymer is simply the sum of the contributions from all the chain segments crossing a unit area of that plane:

$$\sigma(t) = \varrho \sum_{i=1}^{N} \langle \boldsymbol{f}_i \boldsymbol{r}_i \rangle + p\boldsymbol{I} = \varrho k \sum_{i=1}^{N} \langle \boldsymbol{r}_i \boldsymbol{r}_i \rangle + p\boldsymbol{I} \tag{3}$$

where $\varrho = c/N$ is the number of chains per unit volume, c the number of subchains per unit volume, p the pressure arising from van der Waals interactions and kinetic terms, and $\boldsymbol{I}$ the unit tensor. The average $\langle \cdots \rangle$ is to be taken with respect to the non-equilibrium distribution $\Psi(\boldsymbol{r}_1, \ldots \boldsymbol{r}_N, t)$ prevailing at time t. The surrounding chains provide an environment which allows for both RE and CR, and is assumed to be incompressible and to deform affinely. Our treatment will be limited to linear viscoelastic behavior only. For a shear deformation in the x-y plane, the stress is described by the following quantity:

$$\sigma \equiv \sigma_{xy} = \varrho k \sum_{i=1}^{N} \langle x_i y_i \rangle = \varrho k \sum_{i=1}^{N} S_{i,i}(t) \tag{4}$$

where $S_{i,i}$ is the discrete form of the orientation function. The chain is assumed to be initially in equilibrium, with each subchain in its unstressed configuration

$\mathbf{r}_{i,0}$. At $t = 0$ a sudden shear strain γ is imposed on the material and x_i becomes $x_{i0} + \gamma y_{i0}$. The initial stress is therefore:

$$\sigma_{xy}(0) = k\gamma(c/N) \sum_{i=1}^{N} \langle y_{i0}^2 \rangle = k\gamma cr^2/3 = k_B Tc\gamma \tag{5}$$

The time evolution of the stress per unit strain defines the relaxation modulus $G(t)$. As is usual in describing the long-time dynamics of entangled polymer liquids we identify $G(0)$ with the plateau modulus:

$$G(0) = k_B Tc \tag{6}$$

In fact, we expect the initial response to be $G(0) = \alpha k_B Tc$, where α is somewhat less than 1 (it will be taken to be 4/5, [2]) because of relatively rapid initial relaxation by processes other than RE or CR, such as chain contraction within the tube. The long-time behavior of $G(t)$ determines the zero shear viscosity by:

$$\eta = \int_0^\infty G(t)\, dt \tag{7}$$

where

$$G(t) = \sigma_{xy}/\gamma = (\varrho k/\gamma) \sum_{i=1}^{N} S_{i,i}(t) \tag{8}$$

and the recoverable compliance by:

$$J_e = \eta^{-2} \int_0^\infty tG(t)\, dt \tag{9}$$

We therefore seek to evaluate the average quantity $S_{i,i}(t)$.

The time evolution of the N-segment distribution function is governed by an N-dimensional Smoluchowski equation, with anisotropic, orientation-dependent segmental diffusion tensors [3]. Rather than handle this intractable problem directly, we shall write separate equations for RE and CR contributions to $\partial S(i, j; t)/\partial t$, and then sum these to obtain the total rate of change in $S(i, j; t)$ when both mechanisms operate in parallel. In general the resulting $G(t)$ will not be a simple product of RE and CR terms as in the IPM case.

RE term

We derive this term by making the strict reptation assumption, i.e., by forcing each subchain to inherit the position of the preceding or following adjacent subchain with equal probability. As a result $\langle x_i y_j \rangle$ in a single reptation step ($\Delta i = \Delta j = 1$) can become either $\langle x_{i+1} y_{j+1} \rangle$ or $\langle x_{i-1} y_{j-1} \rangle$, i.e., the change in $\langle x_i y_j \rangle$ after an elemental reptative jump can be either equal to $\langle x_{i+1} y_{j+1} \rangle - \langle x_i y_j \rangle$ or $\langle x_{i-1} y_{j-1} \rangle - \langle x_i y_j \rangle$. With this process in mind we write the following difference equation:

$$\partial S_{i,j}/\partial t = (\nu_{RE}/2)(S_{i+1,j+1} + S_{i-1,j-1} - 2S_{i,j}) \tag{10}$$

where ν_{RE} is the jumping frequency for chain motion inside the tube associated with the RE process:

$$\nu_{RE} = \nu_0/N \tag{11}$$

with $\nu_0 = 2k_B T/r^2\zeta_0$ being the subchain jumping frequency, and ζ_0 its friction coefficient. For large N, i and j may be treated as continuum variables, $S_{i,j}(t)$ becomes $S(i, j; t)$, and Eq. (10) may be rewritten as:

$$\partial S(i, j; t)/\partial t = (\nu_{RE}/2)((\partial^2/\partial i^2) + (2\partial^2/\partial i\,\partial j) + (\partial^2/\partial j^2))S(i, j; t) \tag{12}$$

CR term

As stated in the introduction, in the strict reptation picture a chain is surrounded by other neighboring chains which constrain it to move solely along its own contour. The CR hypothesis assumes that vicinal chains are also reptating, and for times comparable to the longest relaxation time of the RE process can move out of the way, thereby adding lateral mobility to the test chain. We model CR as a purely isotropic process that can be described by Rouse-like dynamics. It is important to understand that even though we use Rouse dynamics the physical process being described is not the Rouse process familiar from dilute solution dynamics; in the true Rouse process the "jump frequency" is independent of N but in contrast the CR jump frequency scales as N^{-3}. The CR diffusion equation derived from the Smoluchowski equation is

$$\frac{\partial \Psi(\{\boldsymbol{r}_n\}, t)}{\partial t} = \sum_{n=1}^{N} \frac{\partial}{\partial \boldsymbol{r}_n} \cdot \sum_{m=1}^{N} \frac{A_{nm}}{\zeta}\left[k_B T \frac{\partial \Psi(\{\boldsymbol{r}_m\}, t)}{\partial \boldsymbol{r}_m} + \boldsymbol{f}_m \cdot \Psi(\{\boldsymbol{r}_m\}, t)\right] \tag{13}$$

where A_{nm} is the Rouse matrix:

$$A_{nm} = \begin{cases} 2 & \text{if } n = m \\ -1 & \text{if } n = m+1 \text{ or } m-1 \\ 0 & \text{otherwise} \end{cases} \tag{14}$$

and $\zeta = \zeta_0 N^3$ is the friction factor associated with the CR process, the N^3 dependence reflecting the strict reptation result for the longest relaxation time. Multiplying both sides of the Smoluchowski equation by $x_i y_j$ and by $d^3\boldsymbol{r}$, and averaging over all configuration space, gives:

$$\partial S_{i,j}/\partial t = (\nu_{CR}/2)(S_{i,j+1} + S_{i,j-1} + S_{i+1,j} + S_{i-1,j} - 4S_{i,j}) \tag{15}$$

(i.e., for each CR jump either Δi or Δj is ± 1). In the continuum limit this equation for the pure CR process becomes:

$$\partial S(i, j; t)/\partial t = (\nu_{CR}/2)((\partial^2/\partial i^2) + (\partial^2/\partial j^2))S(i, j; t) \tag{16}$$

where

$$\nu_{CR} = 6k_B T/r^2\zeta = 6k_B T/r^2\zeta_0 N^3 = 3\nu_{RE}/N^2 = 3\nu_0/N^3 \tag{17}$$

is the CR jumping frequency.

PPM model

The right hand side of the difference equation for the PPM is obtained by adding the right hand sides of Eqs. (10) and (16), so that:

$$\begin{aligned}\partial S_{i,j}/\partial t = {} & (\nu_{CR}/2)(S_{i,j+1} + S_{i,j-1} + S_{i+1,j} + S_{i-1,j} - 4S_{i,j}) \\ & + (\nu_{RE}/2)(S_{i+1,j+1} + S_{i-1,j-1} - 2S_{i,j})\end{aligned} \tag{18}$$

We now introduce an effective jump frequency $\alpha(N)$ such that:

$$\nu_{CR}/2 = \alpha(N) \cdot \varepsilon = 3\nu_0/N^3 \tag{19}$$

$$\nu_{RE}/2 = \alpha(N) \cdot (1-\varepsilon) = \nu_0/2N \tag{20}$$

where ε is the constraint release factor ($0 < \varepsilon < 1$). From Eqs. (11) and (17):

$$\alpha(N) = \frac{\nu_0(3+N^2)}{2N^3} \tag{21}$$

and

$$N = [3(1-\varepsilon)/\varepsilon]^{0.5} \tag{22}$$

Note that there exists a unique correspondence between N and ε; $N = 1$ ($\varepsilon = 0.75$) is taken to correspond to M_e, since this molecular weight is the one associated with the appearance of the plateau in $G(t)$. As N increases ε tends to zero, and Eq. (18) tends to the strict RE difference equation. By introducing the dimensionless time variable $\tau = \alpha(N)t$ Eq. (18) is transformed into

$$\begin{aligned}\partial S_{i,j}/\partial\tau = {} & \varepsilon(S_{i,j+1} + S_{i,j-1} + S_{i+1,j} + S_{i-i,j} - 4S_{i,j}) \\ & + (1-\varepsilon)(S_{i+1,j+1} + S_{i-1,j-1} - 2S_{i,j})\end{aligned} \tag{23}$$

the discrete form of the time evolution equation for the PPM model. Equation (23) clearly shows the physical significance of ε, i.e., it is a measure of the contribution of constraint release for a given N. As discussed by Watanabe and Tirrell, the continuum limit of the equation for the PPM process becomes (from Eq. (18)):

$$\begin{aligned}\partial S(i,j;t)/\partial t = {} & \{(\nu_{CR}/2)[(\partial^2/\partial i^2) + (\partial^2/\partial j^2)] \\ & + (\nu_{RE}/2)[(\partial^2/\partial i^2) + 2(\partial^2/\partial i\partial j) + (\partial^2/\partial j^2)]\} S(i,j;t)\end{aligned} \tag{24}$$

The PPM model applies to the post-entanglement regime, where the experimental range is typically $1 < N < 200$; for this reason it is necessary to develop solutions for the discrete version of the model at relatively low N, i.e., to use Eq. (23) rather than Eq. (24), with i and j varying from 0 to $N+1$. The formal addition of subchains 0 and $N+1$ is a convenient way of including the absence of tension felt by the end subchains without writing separate equations for them; the conditions:

$$S_{0,j} = S_{N+1,j} = S_{i,0} = S_{i,N+1} = 0 \tag{25}$$

give the correct equations for subchains 1 and N, and also indicate that these subchains have no preferred orientation. The required initial conditions are:

$$S_{i,j}(0) = (4/5)\gamma\langle y_{i0}^2\rangle = 4\gamma r^2\delta_{ij}/15 \tag{26}$$

where δ_{ij} is the Kronecker delta. Equation (26) represents the random walk configuration of the chain at $t = 0$. Note that even though according to Eq. (5) only the $S_{i,i}(t)$ are required to evaluate the stress, the full two-dimensional problem must be solved to obtain them. Finally, in order to compare this model with Graessley's IPM it is necessary to use the same parameters used by Graessley which are calculated from the Orwoll–Stockmayer random bond flip mechanism, as described in the Appendix.

3. Results

Continuum limit approximation

The quantity of interest is the subchain orientation correlation function, $S(i, j; t)$, where i and j are continuous subchain index variables that identify positions along the chain and run from 1 to N; its time evolution is given by Eq. (24) with the initial conditions:

$$S(i, j; 0) = 4\gamma r^2 \delta(i - j)/15 \tag{28}$$

where $\delta(i - j)$ is the Dirac delta function, and boundary conditions:

$$S(0, j; t) = S(N, j; t) = S(i, 0; t) = S(i, N; t) = 0 \tag{29}$$

Watanabe and Tirrell solved the PPM in the continuum limit, treating the time evolution of $S(i, i; t)$ as occurring through a sequence of alternating RE and CR steps, using approximate expressions for $S(i, i; t)$ during the CR phases [13]. Here a numerical approach to the continuum problem (finite differences) has been chosen instead, starting at the $S(i, j; t)$ level. Equation (24) is replaced by a difference equation for $S_{m,n}(t)$, similar to Eq. (23) with a P by P grid of mesh length $\Delta m = \Delta n = N/P < 1$, where P is made sufficiently large to provide convergence and is kept constant and therefore independent of N [16]

$$\begin{aligned} \partial S_{m,n}/\partial \tau = {} & \varepsilon(S_{m,n+1} + S_{m,n-1} + S_{m+1,n} + S_{m-1,n} - 4S_{m,n}) \\ & + (1 - \varepsilon)(S_{m+1,n+1} + S_{m-1,n-1} - 2S_{m,n}) \end{aligned} \tag{23'}$$

where the dimensionless time variable in Eq. (23) is now $\tau = \alpha(N)(N/P)^2 t$. When $P = N$ the difference equation becomes identical with Eq. (23); however, to attain the continuum limit P must be kept large compared to N. It should be noted that in the finite differences scheme Eqs. (28) and (29) become:

$$S_{m,n}(0) = (4N/15P)\gamma r^2 \delta_{mn} \quad 0 < m, n < P \tag{28'}$$

so that the initial stress remains independent of P, and

$$S_{0,n} = S_{N+1,n} = S_{m,0} = S_{m,N+1} = 0 \quad 0 < m, n < P \tag{29'}$$

respectively, where division by P ensures that the sum of diagonal elements at time zero is $(4/15)N\gamma r^2$.

The numerical results differ significantly from Watanabe and Tirrell's solution. As an example, Fig. 2 compares both the Watanabe–Tirrell and the numerical continuum limit approximation predictions for η with the strict RE predictions as well as with experiment for narrow M distribution polystyrene at 167°C [17]. As the molecular weight increases, there is a convergence to the strict RE results in Watanabe and Tirrell's calculations. This can be interpreted to mean that at higher N the frequency of release of a constraint is so low compared to the reptative jump frequency that RE is the only contributing relaxational possibility for the chain. However, no evidence of convergence to pure RE is observed for the numerical calculations in the range of N examined. It is interesting to note that in the region of interest the molecular weight exponent of the viscosity is a function of molecular weight and has a value greater than 3, in both cases. This exponent can be reasonably well approximated by 3.6, close to the value found experimentally, for Watanabe and Tirrell's predictions but the numerical predictions exhibit a value of approximately 4.1.

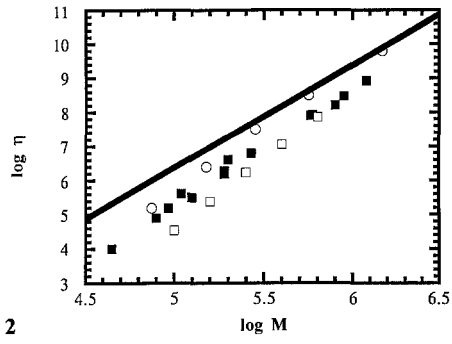
log η
log M
11
10
9
8
7
6
5
4
3
4.5
5
5.5
6
6.5

2

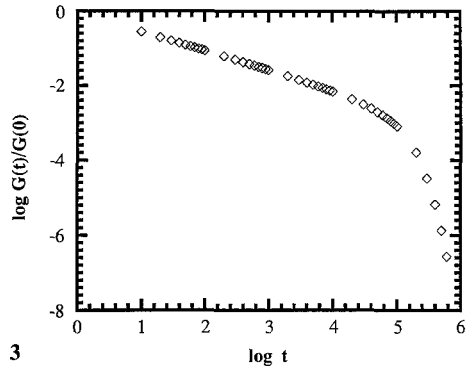
log G(t)/G(0)
log t
0
-2
-4
-6
-8
0
1
2
3
4
5
6

3

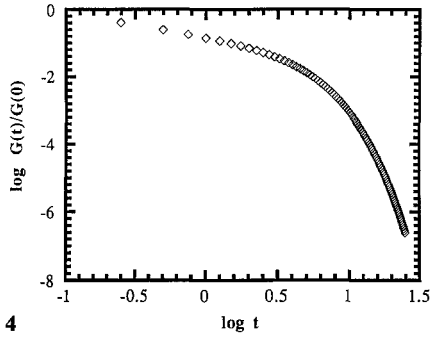
log G(t)/G(0)
log t
0
-2
-4
-6
-8
-1
-0.5
0
0.5
1
1.5

4

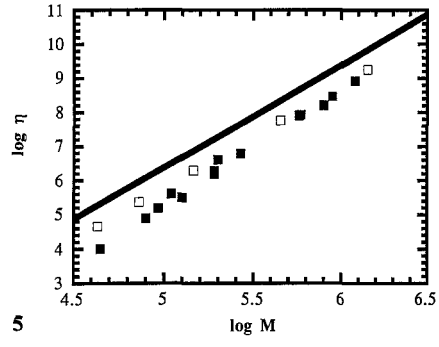
log η
log M
11
10
9
8
7
6
5
4
3
4.5
5
5.5
6
6.5

5

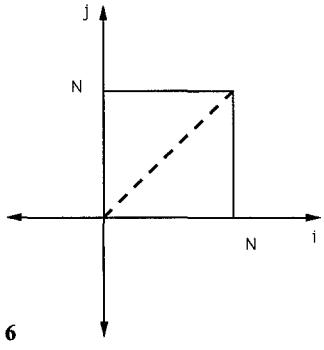
j
N
N
i

6

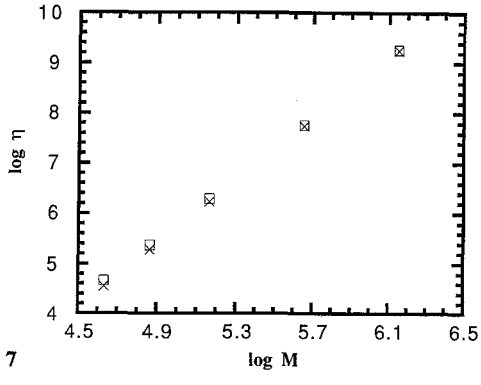
log η
log M
10
9
8
7
6
5
4
4.5
4.9
5.3
5.7
6.1
6.5

7

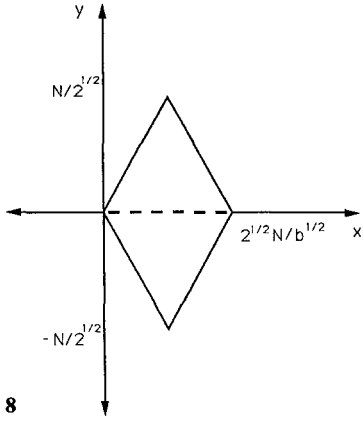
y
N/2^1/2
2^1/2N/b^1/2
x
-N/2^1/2

8

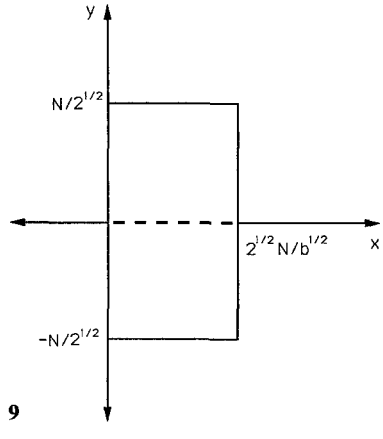
y
N/2^1/2
2^1/2N/b^1/2
x
-N/2^1/2

9

Finally, while the numerical results underestimate the magnitude of the experimental data Watanabe and Tirrell's predictions do the opposite, as pointed out by these authors [13]. The differences between the two continuum results are presumably attributable to the diagonal dominance approximation and an initial condition (different from Eq. (28)):

$$S(i,j;0) = \begin{cases} (4/15)\gamma r^2 & \text{for } |i-j| < 1 \\ 0 & \text{for } |i-j| < 1 \end{cases} \tag{30}$$

used by Watanabe and Tirrell. Some preliminary calculations of the solution to Eq. (24) using the initial condition of Eq. (30) have yielded results different from the continuum limit results both with the diagonal dominance approximation and the numerical solution presented here [18]. If Eq. (23) is considered as a purely mathematical problem then ε can be allowed to go to zero and the strict RE result is recovered, regardless of the value of P used. Of course, this result has no physical meaning in the context of the PPM because the convergence to strict RE will not be achieved before ε becomes so small that N will be greater than P and application of the continuum limit approximation is no longer appropriate since the $P \gg N$ requirement has been violated.

The discrete case

As mentioned earlier, $N = M/M_e$, and experimentally N extends from 1 to 200, thus warranting an examination of the discrete result. First, however, it is

---

Fig. 2. Molecular weight dependence of the viscosity. Comparison of the strict RE prediction (from the solution of Eq. (10)) (*thick line*), Watanabe and Tirrell's continuum limit results (*open circles*), and the numerical continuum limit results (*open squares*) with PS of narrow molecular weight distribution experimental data (*filled squares*), taken from Ref. [17]

Fig. 3. Time dependence of $G(t)/G(0)$ as predicted by the continuum Rouse model showing the intermediate $t^{-1/2}$ scaling

Fig. 4. Time dependence of $G(t)/G(0)$ as predicted by the discrete Rouse model for $N = 5$ showing no evidence of an intermediate $t^{-1/2}$ scaling

Fig. 5. Molecular weight dependence of the viscosity. Comparison of the strict RE prediction (from the solution of Eq. (10)) (*thick line*) and the numerical discrete PPM results (*open squares*) with PS of narrow molecular weight distribution experimental data (*filled squares*), taken from Ref. [17]

Fig. 6. Projection of $S(i,j;\tau)$ or "mass distribution" function (in the diffusion equation analogy case) onto the i-j plane at $\tau = 0$. As time evolves the initial mass distribution (which projects onto the $i = j$ diagonal) is depleted and the "mass", in this figure the projection of its distribution, spreads within the square and is absorbed if it reaches the boundaries

Fig. 7. Molecular weight dependence of the viscosity. Comparison of the numerical discrete PPM results (*open squares*) with Graessley's IPM results (*crosses*)

Fig. 8. Projection of $S(x,y;\tau)$ or "mass distribution" function (in the diffusion equation analogy case) onto the x-y plane at $\tau = 0$. As time evolves the initial mass distribution (which projects onto the $y = 0$ line) is depleted and the "mass", in this figure the projection of its distribution, spreads within the diamond (resulting from the change of variables) and is absorbed if it reaches the boundaries

Fig. 9. Representation of the Fig. 8 case with new boundaries necessary to generate an IPM solution to the problem

instructive to examine the differences between the continuum limit approximation and the discrete solution for a simpler model, the Rouse model [3, 4, 19]. This model is of relevance to this work because it is mathematically identical to the CR model, i.e., it is described by the same differential equation and initial and boundary conditions. One of the best known results of the continuum limit approximation of the Rouse model is the $t^{-1/2}$ dependence of the relaxation modulus, as illustrated in Fig. 3. However, when the discrete problem is solved for a Rouse chain of 5 subchains there is no evidence of such time scaling, as shown in Fig. 4, since the continuum view is not applicable to short chains.

We now proceed to examine the solution to Eqs. (23, 25 and 26). The results for the molecular weight dependence of the viscosity are shown in Fig. 5, where we also show the strict RE result and compare to experiment. These results are significantly different from the continuum limit approximation results. Surprisingly, the viscosity exponent is 3, just as in the strict RE case, and the inclusion of the CR mechanism only affects the viscosity prefactor. As in the continuum limit (numerical solution) no convergence to strict RE is observed in the range of N examined; however, the magnitude of the viscosity is overestimated. The differences between the continuum limit and discrete numerical PPM predictions are due to the fact that in the former each subchain is being divided into P/N subunits, in effect providing non-existent additional internal mechanisms for relaxation.

To solve Eqs. (23, 25, and 26), which are stochastic difference equations, we represent the spatial part of the problem as an N by N numerical grid; in this case the grid does have physical significance, because its size will directly depend on the molecular weight of the chain being modeled ($P = N$). These equations have the appearance of anisotropic diffusion equations, where the "mass distribution" (or correlation function in this case) at any time is a distribution over the i-j plane, as illustrated in Fig. 6. It is important to remember, however, that no physical diffusion process is involved, and that the diffusion-like terms are a result of the Hookean interactions between adjacent beads. Nevertheless, we can use this diffusion analogy to describe the relaxation mechanism of the PPM model. At time $t = 0$ the "diffusing material" is distributed along the diagonal $i = j$, with absorbing boundaries at i or j equal to 0 or $N + 1$. If the system can only relax its orientation via RE, "mass" can only be lost at either end of the diagonal. On the other hand, if the system can also relax via CR, the "mass" can "diffuse" at right angles to its original distribution and can ultimately be absorbed at any point on the boundary of the i-j plane. These two competing relaxation mechanisms may be called longitudinal and transverse respectively. For a chain of $N = 4$, the efficiency of orientation relaxation of both mechanisms is similar because the system has two end beads and two internal beads. As N becomes greater, the transverse or CR mechanism becomes more effective (relative to the longitudinal or RE mechanism) at relaxing stress because the fraction of internal subunits increases, in other words, the possibilities per unit time for relaxation along the diagonal increase as N increases whereas the number of possibilities at the ends remain fixed. However, as N becomes larger the frequency of release of a constraint becomes lower and ε becomes smaller, thereby limiting the effectiveness of the transverse mechanism and allowing the longitudinal RE relaxation mechanism to dominate. The balancing of these two effects is sufficient to impede a convergence to RE in the region of N examined, even though the CR process weighting is being reduced. Physically the discrete

results can be interpreted in the following way: chains can relax via RE only at the ends and via CR anywhere along their own contour, so that as N becomes larger the frequency of release of a constraint decreases but the contour of the chain increases providing more possibilities along the chain for a constraint to be released. As $N \to \infty$ and $\varepsilon \to 0$ it is clear from Eq. (23) that the strict RE result must be recovered; however, based on the numerical PPM results it is evident that this convergence is very slow, and not visible in the region of N examined.

Figure 5 reveals one of the weaknesses of the rigorous, discrete solution of the PPM namely that, since experimentally the viscosity has a stronger molecular weight dependence, the experimental and theoretical curves will cross each other and the model will underestimate the experimental data at high M.

Independent processes solution

As explained in the introduction this model, due to Graessley, is based on the assumption that the relaxation modulus can be expressed as the simple product $G(t)/G(0) = G_{CR}(t)G_{RE}(t)$ [5]. This assumption can be rationalized in the following way: the jump frequencies for the CR and RE processes scale as N^{-3} and N^{-1}, respectively, and thus the ratio of the characteristic frequencies for both processes scales as N^{-2} for the monodisperse case. Hence, at sufficiently high molecular weights the time scales of the processes are well separated. Figure 7 shows a comparison between this model and the rigorous discrete result of the PPM. For the viscosity Graessley's model is clearly a very good approximation. It should be noted, however, that this is not true for all properties; for example the end-to-end vector correlation function, $V(t) = \langle \boldsymbol{R}(t) \cdot \boldsymbol{R}(0) \rangle$, where $\boldsymbol{R}(t)$ is the end-to-end vector, predicted by the PPM model is in better agreement with experiment than Graessley's model, as discussed by Watanabe and Tirrell [13]. Calculation of $V(t)$ does not require the use of DDA and therefore the differences between the models, which are a result of using the DDA approximation or different initial conditions, i.e., Eqs. (28) and (30), do not arise.

In order to understand the agreement between Graessley's result and the rigorous discrete result, an independent processes solution is derived in the framework of reptation plus constraint release with Eqs. (24, 28, and 29) as the starting point. After a change of variables to

$$\tau = t\nu_{CR}, \qquad y = 2^{-1/2}(i-j) \quad \text{and} \quad x = (2\beta)^{-1/2}(i+j), \tag{31}$$

where $\beta = 1 + 2\nu_{CR}/\nu_{RE}$, Eq. (23) becomes:

$$\partial S(x, y, \tau)/\partial\tau = \left(\frac{\partial^2}{\partial x^2} + \frac{\partial^2}{\partial y^2}\right) S(x, y, \tau) \tag{32}$$

with

$$\begin{aligned} S(x = -y\beta^{-1/2}) = S(x = y\beta^{-1/2}) = S(y + x\beta^{1/2} = 2^{1/2}N) \\ = S(-y + x\beta^{1/2} = 2^{1/2}N) = 0 \end{aligned} \tag{33}$$

as boundary conditions and

$$S(x, y, 0) = (2\beta)^{1/2} r^2 \delta(2^{1/2}y) 4/15 \tag{34}$$

as an initial condition. Figure 8 shows the transformation from the i-j plane to the x-y plane, with the boundaries forming an elongated diamond shape and all

the "mass" distributed along $y = 0$. Now "mass" can "diffuse" out at $x = 0$ or $x = \beta^{-1/2}2^{1/2}N$ by reptation or perpendicular to $y = 0$ by CR. At short or intermediate times the vertices of the diamonds are not having any effect and the boundaries can be replaced by straight lines perpendicular to the x-axis. As illustrated in Fig. 9:

$$S(x = 0) = S(x = \beta^{-1/2}2^{1/2}N) = S(y = 2^{-1/2}N) = S(y = -2^{-1/2}N) = 0 \quad (35)$$

are the new boundary conditions. Under these conditions the problem becomes separable and the solution is a product of the solutions to the x and y parts of the problem, where the y part is a CR-like function and the x part is a RE-like function. Thus, we recover an IPM solution. The fact that both models give very similar results can be interpreted to mean that for times that are sufficiently long for the diffusing mass to "feel" the differences between the two kinds of boundaries, most of the initial mass distribution has been depleted.

The recoverable compliance

The product $J_eG(0)$ gives a measure of the breadth of the distribution of relaxation modes. The following table shows this product for different N as predicted by Graessley's model and the discrete PPM, with $z = 3.5$, and by the continuous PPM, with the DDA and $z = 3.0$. In all cases $J_eG(0)$ becomes independent of N at high N; however, the continuous PPM with the DDA converges to the strict RE prediction of 6/5 while the other two models predict higher values. Also, the discrete PPM and Graessley's model approach the N-independent value of $J_eG(0)$ from below while the continuous PPM with the DDA approaches from above. The experimental value of this product is independent of M and lies between 2 and 3 [20].

Table of predictions for $J_eG(0)$ as a function of N

N	Graessley ($z = 3.5$)	PPM-discrete ($z = 3.5$)	PPM-DDA ($z = 3.0$)
10	2.18	1.96	1.41
30	2.33	2.13	1.28
100	2.37	2.32	1.22
150	2.37	2.32	1.22

4. Conclusion

The parallel processes model for combined reptation and constraint release has been derived and solved numerically by finite differences starting at the orientation correlation function level. The results presented here focus on the molecular weight dependence of the viscosity. In the continuum approximation the viscosity exponent is greater than 3 and depends on the molecular weight, a crossover to strict reptation is not observed and the magnitude of the viscosity is underestimated. The discrete solution, which is appropriate for experimentally accessible molecular weights, exhibits very different qualitative features. Surprisingly the

exponent is 3, just as in the RE case, the viscosity is overestimated and no crossover to strict reptation is observed in the region of molecular weight investigated. Inclusion of the constraint release mechanism merely lowers the viscosity prefactor, which is one of the weaknesses of the parallel processes model, since the stronger experimental molecular weight dependence will eventually result in an underestimation of experimental results. The independent processes model is shown to be a good approximation to the parallel processes model for the viscosity; however this is not the case for the end-to-end vector correlation function. It is clear that linear combinations of reptation and constraint release, as modeled here, cannot describe the viscosity results observed experimentally and further refinement of the model is required.

Acknowledgements. Financial support for this work was provided by the Petroleum Research Fund (American Chemical Society), the Rohm and Haas Company, and the Minnesota Supercomputer Institute.

Appendix

The Orwoll–Stockmayer (OS) random bond flip mechanism was incorporated by Graessley to account for the change in chain configuration following the release of a constraint. This event is referred to as a local jump, and in the framework of the OS model it is assumed that the average number of properly positioned constraints per subunit, or tube segment, is z. The characteristic frequency for the CR process changes from that in Eq. (18) to:

$$\nu_{CR} = \alpha(N) \cdot \varepsilon = 3\nu_0\pi^2/N^3 12\Lambda(z) \tag{A1}$$

where $\Lambda(z) = (1/z)(\pi^2/12)^z$, and Eqs. (21) and (22) change accordingly. Physically, a greater z, which implies a higher ν_{CR}, results in a greater contribution of the CR process for a given N. Comparison with experiment can be carried out, following Doi and Edwards, by using the Rouse relation $r^2\zeta_0 k_B T = 144\eta(M_c)/5G(0)N_c$, where $\eta(M_c)$ is the viscosity at the critical molecular weight M_c, $N_c = M_c/M_e$, $M_e = 4cRT/5G(0)$, R is the universal gas constant, and z is the only parameter left to be determined. This parameter has been found experimentally to be approximately 3.5 [13]. The viscosity is finally given by:

$$\eta = \frac{(N/P)^2 G(0)}{\frac{\nu_0}{2}\left(\frac{3\pi^2}{N^3 12\Lambda(z)} + \frac{1}{N}\right)} \int_0^\infty F(\tau)\, d\tau \tag{A2}$$

where

$$F(\tau) = \sum_{i=1}^{P} S'_{i,i}(\tau) \tag{A3}$$

and

$$S'_{i,i}(\tau) = \frac{4P\gamma r^2 S_{i,i}(\tau)}{15N \sum_{i=1}^{P} S_{i,i}(0)} \tag{A4}$$

which is the function calculated numerically. It should be noted that in the discrete case P is replaced by N.

References

1. de Gennes PG (1971) J Chem Phys 55:572
2. Doi M, Edwards SF (1978) J Chem Soc, Faraday Trans 2 74:1789, 1802, 1818 75:38
3. Doi M, Edwards SF (1989) The theory of polymer dynamics. Oxford Univ Press, Oxford, UK
4. Lodge TP, Rotstein NA, Prager S (1990) Adv Chem Phys 79:1
5. Graessley WW (1982) Adv Polym Sci 47:68
6. Yoshida H, Watanabe H, Kotaka T (1991) Macromolecules 24:572
7. Struglinski MJ, Graessley WW (1986) Macromolecules 18:2630
8. Rubinstein M, Colby RH (1988) J Chem Phys 89:5291
9. Green PF, Kramer EJ (1986) Macromolecules 19:1108
10. Antonietti M, Coutandin J, Sillescu H (1986) 19:793
11. Klein J (1978) Macromolecules 11:852
12. Daoud M, de Gennes PG (1979) J Polym Sci, Polym Phys Ed 17:1971
13. Watanabe H, Tirrell M (1989) Macromolecules 22:927
14. Doi M (1983) J Polym Sci, Polym Phys Ed 21:667
15. Graessley WW (1980) J Polym Sci, Polym Phys Ed 18:27
16. Hildebrand FB (1968) Finite difference equations and simulations. Prentice-Hall, Englewood Cliffs, NJ
17. McKenna GB, Hadziioannou G, Lutz P, Hild G, Strazielle C, Straupe C, Rempp P, Kovacs AJ (1987) Macromolecules 20:498
18. Watanabe H (1991) personal communication
19. Rouse PE (1953) J Chem Phys 21:1272
20. Compliance data for PS are reported in: Odani H, Nemoto N, Kotaka M (1972) Bull Inst Chem Res Kyoto Univ 50:117